Astronomy
&
Astrophysics

Hα surface photometry of galaxies in the Virgo cluster

IV. The current star formation in nearby clusters of galaxies[*,**]

G. Gavazzi[1], A. Boselli[2], P. Pedotti[1], A. Gallazzi[1], and L. Carrasco[3,4]

[1] Università degli Studi di Milano-Bicocca, Piazza delle scienze 3, 20126 Milano, Italy
    e-mail: giuseppe.gavazzi@mib.infn.it
[2] Laboratoire d'Astrophysique de Marseille, Traverse du Siphon, 13376 Marseille Cedex 12, France
    e-mail: Alessandro.Boselli@astrsp-mrs.fr
[3] Instituto Nacional de Astrofísica, Optica y Electrónica, Apartado Postal 51. C.P. 72000 Puebla, Pue., México
    e-mail: carrasco@transun.inaoep.mx
[4] Observatorio Astronómico Nacional, UNAM, Apartado Postal 877, C.P. 22860, Ensenada B.C., México

Abstract. Hα+[NII] imaging observations of 369 late-type (spiral) galaxies in the Virgo cluster and in the Coma/A1367 super-cluster are analyzed, covering 3 rich nearby clusters (A1367, Coma and Virgo) and nearly isolated galaxies in the Great-Wall. They constitute an optically selected sample ($m_p < 16.0$) observed with ~60% completeness. These observations provide us with the current ($T < 10^7$ yrs) star formation properties of galaxies that we study as a function of the clustercentric projected distances (Θ). The expected decrease of the star formation rate (SFR), as traced by the Hα EW, with decreasing Θ is found only when galaxies brighter than $M_p \sim -19.5$ are considered. Fainter objects show no or reverse trends. We also include in our analysis Near Infrared data, providing information on the old ($T > 10^9$ yrs) stars. Put together, the young and the old stellar indicators give the ratio of currently formed stars over the stars formed in the past, or "birthrate" parameter b. For the considered galaxies we also determine the "global gas content" combining HI with CO observations. We define the "gas deficiency" parameter as the logarithmic difference between the gas content of isolated galaxies of a given Hubble type and the measured gas content. For the isolated objects we find that b decreases with increasing NIR luminosity. In other words less massive galaxies are currently forming stars at a higher rate than their giant counterparts which experienced most of their star formation activity at earlier cosmological epochs. The gas-deficient objects, primarily members of the Virgo cluster, have a birthrate significantly lower than the isolated objects with normal gas content and of similar NIR luminosity. This indicates that the current star formation is regulated by the gaseous content of spirals. Whatever mechanism (most plausibly ram-pressure stripping) is responsible for the pattern of gas deficiency observed in spiral galaxies members of rich clusters, it also produces the observed quenching of the current star formation. A significant fraction of gas "healthy" (i.e. with a gas deficiency parameter less than 0.4) and currently star forming galaxies is unexpectedly found projected near the center of the Virgo cluster. Their average Tully-Fisher distance is found approximately one magnitude further away ($\mu_o = 31.77$) than the distance of their gas-deficient counterparts ($\mu_o = 30.85$), suggesting that the gas healthy objects belong to a cloud projected onto the cluster center, but in fact lying a few Mpc behind Virgo, thus unaffected by the dense IGM of the cluster.

Key words. galaxies: photometry – galaxies: clusters: individual: Virgo

1. Introduction

A significant trend of the global star formation rate (SFR) of galaxies with the projected clustercentric distance from rich clusters of galaxies is well documented in the local universe ($0.05 < z < 0.1$). The mean SFR, as traced by the equivalent width of the Hα line (Kennicutt 1989), is found to decrease with decreasing distance from rich clusters (Lewis et al. 2002). This pattern is dominated by the "morphology segregation" effect (Dressler 1980), i.e. there are more elliptical and spheroidal galaxies with little or no current star formation than the star forming galaxies in the center of rich clusters. What physical mechanism (nature vs. nurture) is responsible for the morphological transformation taking place in the densest environments is however not yet fully understood. To shed light on the various possibilities, i.e. galaxy harassment (Moore et al. 1996, 1998), tidal stirring (Mayer et al. 2001) or ram pressure stripping (Gunn & Gott 1972), it is crucial to establish observationally if, beside the morphology segregation, galaxies of

a given morphological type, namely the spirals, are affected by a systematic SFR decrease toward the center of nearby clusters.

If on the one hand Kennicutt (1983) found that spirals in the Virgo cluster have their mean SFR as much as a factor of two lower than isolated galaxies, Gavazzi et al. (1998) did not confirm this evidence in the Coma and A1367 clusters. Moreover Iglesias-Paramo et al. (2002) found that the shape of the Hα luminosity function of these two clusters does not differ significantly from the one of isolated galaxies. The result of Kennicutt (1983) was based on only a dozen giant galaxies with Hα measurements from aperture photometry, thus requiring a confirmation on a larger sample with modern imaging data.

With the aim of solving this riddle we undertook an Hα imaging survey of two optically complete samples of galaxies. The first is composed of nearly isolated objects selected from the CGCG (Zwicky et al. 1961–68) in the bridge between Coma and A1367, which we observed down to the limit of 15.7 mag. This constitutes our reference sample of noncluster objects. The cluster sample is focused on A1367, the Coma and the Virgo clusters. We took Hα imaging observations of these regions (Gavazzi et al. 1998; Gavazzi et al. 2002a, Paper I of this series; Boselli & Gavazzi 2002, Paper II; Boselli et al. 2002b, Paper III). Our own observations were complemented with data taken from the literature (Kennicutt & Kent 1983; Romanishin 1990; Gavazzi et al. 1991; Young et al. 1996; Koopmann et al. 2001).

Furthermore we performed a NIR imaging survey of the same regions (Gavazzi et al. 2000b and references therein), providing information on the old stars.

In the present paper we combine Hα with NIR measurements to study the young and the old components of the stellar population integrated over the whole galaxy and we analyze the properties of the stars as a function of the clustercentric projected distance, of the luminosity and of the global gas content. We postpone to a forthcoming paper the morphological aspects of the analysis related to the spatial distribution of the young/old stars. The present paper is organized as follows: in Sect. 2 we briefly present the new Hα imaging observations of 13 galaxies. The sample used in the present investigation is illustrated in Sect. 3. After defining the "birth-rate" parameter (Sect. 4.1) and the "gas-deficiency" parameter (Sect. 4.2), we analyze in Sect. 5.1 the clustercentric dependence of the current star formation rate. In Sects. 5.2 and 5.3 we study the current star formation properties of galaxies in 3 local clusters as a function of their global luminosity and gaseous properties. The conclusions are briefly discussed in Sect. 6 and summarized in Sect. 7.

2. New observations

Narrow band imaging in the Hα emission line ($\lambda = 6562.8$ Å) of 13 galaxies was obtained in March 20, 2002, using the 2.1 m telescope at San Pedro Martir Observatory (SPM) (Baja California, Mexico).

The target galaxies are listed in Table 3 as follows:

- Column 1: VCC (Binggeli et al. 1985) or CGCG (Zwicky et al. 1961–68) designation.

- Column 2: NGC/IC name.
- Column 3: UGC name.
- Columns 4 and 5: J2000 celestial coordinates.
- Column 6: photographic magnitude as given in the VCC or in the CGCG.
- Column 7: heliocentric velocity (km s^{-1}) from the VCC or from Gavazzi et al. (1999a).
- Column 8: exposure times in minutes for the ON-band filter.
- Column 9: transmissivity ($R_{\rm ON}$) of the ON-band filter at the redshifted Hα line.

We used a Site 1024 × 1024 pixels CCD detector with pixel size of 0.31 arcsec. Each galaxy was observed through a narrow band interferometric filter (~90 Å width) centered at λ 6603, for the galaxies at the redshift of Virgo (350 < V < 3000 km s^{-1}), and at λ 6723 Å, for galaxies in the Coma supercluster. These observations provided us with the ON-band images and required 15–20 min integration time. The OFF-band images were obtained through the r-Gunn filter and were exposed one fifth of the ON-band ones. The observations were obtained with the seeing ranging from 1.2 to 3 arcsec, but in photometric conditions. They were flux calibrated using the standard stars Feige 34 and Hz44 from the catalogue of Massey et al. (1988), observed every 2 hours. Repeated measurements gave <0.05 mag differences, which we assume as the typical uncertainty (1σ) of the photometric results given in this work.

The reduction of the CCD frames follows a procedure identical to the one described in previous papers of this series (e.g. Gavazzi et al. 2002), based on the IRAF STSDAS[1] reduction packages, and it will be briefly summarized here. To remove the detector response each image was bias subtracted and divided by the median of several flat field exposures obtained on empty regions of the twilight sky. Cosmic rays were removed either using the task COSMICRAY in IRAF or manually by direct inspection of the frames. The sky background was determined in each frame in concentric object-free regions around the galaxies and then subtracted from the flat-fielded images. The typical uncertainty on the mean background is estimated 10% of the rms in the individual pixels. This represents the dominant source of error in low S/N regions.

Hα fluxes and equivalent widths are estimated subtracting the contribution of the continuum from the ON-band measurements. As the continuum was estimated using the broad band r filter, which in fact includes the Hα and [NII] lines, the corrected fluxes and equivalent widths are computed according to Eqs. (1) and (2) of Paper III, and their uncertainties are given by:

$$\sigma_{F_c} = \sigma_F \left(1 + \frac{\int R_{\rm ON}(\lambda)\mathrm{d}\lambda}{\int R_{\rm OFF}(\lambda)\mathrm{d}\lambda}\right) \tag{1}$$
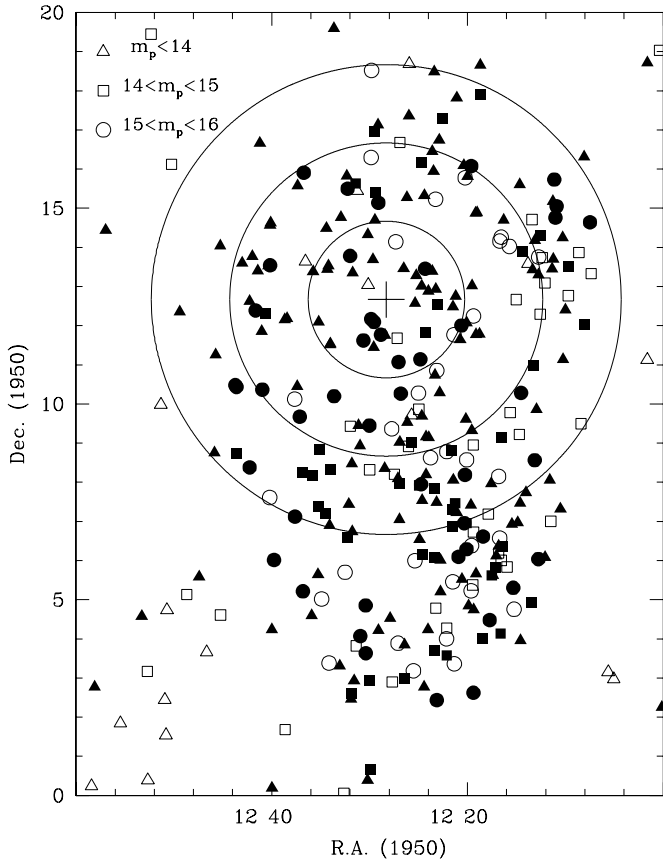
Fig. 1. Sky distribution of the 312 spiral galaxies brighter than $m_p \leq 16.0$ in the VCC. The filled symbols represent 235 galaxies with available Hα data, the empty ones to unobserved galaxies. Circles are drawn at 2, 4, 6 deg projected radial distance from M 87 (cross).

$$\sigma_{EW_c} = \sigma_{EW}\left(1 + \frac{\int R_{ON}(\lambda)d\lambda}{\int R_{OFF}(\lambda)d\lambda}\right) \times \left(\frac{1}{1 - \left(\frac{EW}{\int R_{OFF}(\lambda)d\lambda}\right)^2}\right). \qquad (2)$$

Galaxies with substantial Hα + [NII] structure are given in Fig. 14. The contours of the OFF frames are superposed to the NET (ON-OFF) frames (grey-scale).

3. The sample

Including the new observations presented in this paper, this work comprises Hα and NIR (H band) imaging observations of 369 late-type galaxies belonging to the Virgo cluster and to the Coma supercluster region.

The Virgo cluster galaxies were selected from the Virgo Cluster Catalogue (VCC) of Binggeli et al. (1985), with $m_p \leq 16.0$, Hubble type later than S0a (as given in the VCC) and classified as cluster members, possible members or belonging to the W, W', M clouds or to the southern extension (Binggeli et al. 1985, 1993; see also Gavazzi et al. 1999a) matching $V < 3000$ km s^{-1} (see Fig. 1).

The late-type ($> S0a$) galaxies in the Coma supercluster region ($18^o \leq \delta \leq 32^o$; $11.5^h \leq \alpha \leq 13.5^h$) were selected from the CGCG catalogue ($m_p \leq 15.7$) (Zwicky et al. 1961–68) and include members to the Coma Supercluster according to
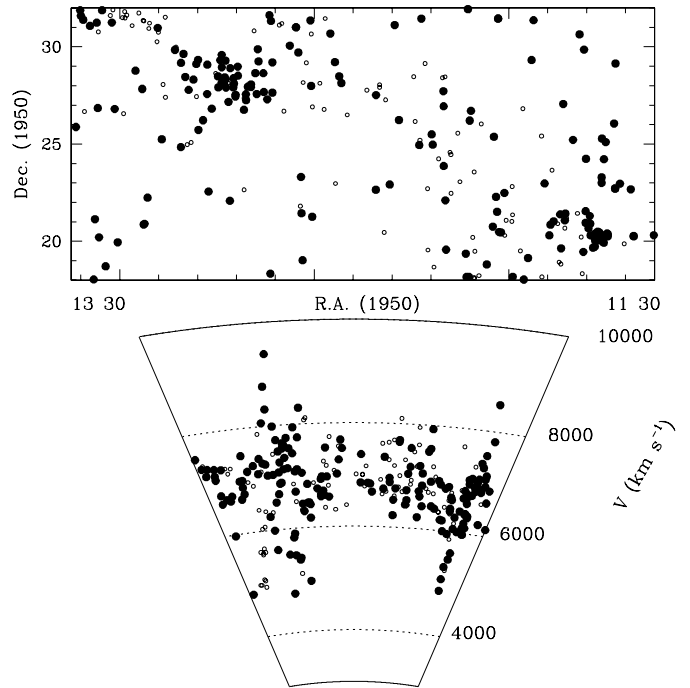

Fig. 2. Sky distribution of the 256 spiral galaxies brighter than $m_p \leq 15.7$ in the CGCG in the Coma supercluster region (top). Wedge diagram (bottom). The filled symbols represent 158 galaxies with available Hα data, the empty ones to unobserved galaxies.

Gavazzi et al. (1999b) (see Fig. 2). Table 1 gives the details of the sample completeness in the two studied regions. The Coma supercluster members are divided in cluster (A1367+A1656) members, members to groups and pairs (see Gavazzi et al. 1999b) and strictly isolated supercluster objects (with projected separations >300 kpc). The Hα observations were taken either from the present series of papers (Papers I, II, III, IV, primarily devoted to the Virgo cluster), from Gavazzi et al. (1991, 1998) (containing mostly observations of the Coma supercluster region) or from Kennicutt & Kent (1983), Kennicutt et al. (1984), Romanishin (1990), Koopmann et al. (2001) (see detailed references in Table 4).

The NIR observations were taken from the series of papers "Near-infrared H surface photometry of galaxies" (Gavazzi et al. 1996a,b, 2000a; Boselli et al. 1997; Boselli et al. 2000 and from Gavazzi et al. 2001). Total asymptotic H band magnitudes were obtained by Gavazzi et al. (2000b) and by Gavazzi et al. (2001).

As listed in Table 1 the combined NIR+ Hα observations cover more than 60% of the targets in all regions (except Coma supercluster groups+pairs), thus our data can be considered as representative of the late-type galaxies in the studied regions.

The analyzed galaxies are listed in Table 4 as follows:

– Column 1: VCC designation, from Binggeli et al. (1985) for Virgo galaxies, or CGCG (Zwicky et al. 1961–68) for Coma supercluster galaxies.
– Column 2: the membership to a cluster or supercluster, defined as in Gavazzi et al. (1999a) for Virgo and Gavazzi et al. (1999b) for the Coma/A1367 supercluster.

Table 1. The sample completeness.

region	$m_p \leq 16.0$	with NIR	with NIR & H$_\alpha$	Compl.
Virgo	323	271	205	63%
Coma S. (Clusters)	72	72	54	75%
Coma S. (Grps+Prs)	67	67	27	40%
Coma S. (Isolated)	119	83	83	69%
Tot.	568	480	356	63%

- Column 3: morphological type as given in the VCC or in Gavazzi & Boselli (1996).
- Column 4: projected angular separation from the nearest cluster center (degrees).
- Column 5: asymptotic *H* band magnitude, obtained as described in Gavazzi et al. (2000b).
- Column 6: distance (Mpc); we assume 17 Mpc for Virgo A, N, S, E, 23 Mpc for Virgo B and 32 Mpc for Virgo W, M as given in Gavazzi et al. (1999a), 96 Mpc for Coma, 91 Mpc for A1367. For galaxies not belonging to the clusters, the distance is determined from the redshift using $H_0 = 75$ km s^{-1} Mpc^{-1}.
- Column 7: gas deficiency parameter as defined in Sect. 4.2.
- Column 8: H$_\alpha$ + [NII]EW(Å).
- Column 9: Log of the H$_\alpha$ flux (erg cm^{-2} s^{-1}) deblended from the [NII] contribution and corrected for internal extinction as in Boselli et al. (2001).
- Column 10: reference to the H$_\alpha$ data (as listed at the bottom of the table).

4. Tools

4.1. The birthrate parameter

H$_\alpha$ and NIR observations provide us with information on stellar populations with different time scales: $\sim 10^7$ yrs the former and $\sim 10^{10}$ yrs the latter. The two quantities combined give the ratio of the current SFR to the average past SFR or the birthrate parameter b, as defined by Kennicutt et al. (1994).

Following Boselli et al. (2001), we use the Near Infrared luminosity L_H as a tracer of the global mass of old stars, assuming that disk galaxies have a constant $M_{Tot}/L_H = 4.6$ within their optical radius (Gavazzi et al. 1996c). Thus we write the adimensional parameter b as:

$$b_{obs} = \frac{SFR \, t_o \, (1 - R)}{L_H \, (M_{Tot}/L_H) \, DM_{cont}} \tag{3}$$

where SFR is derived from the H$_\alpha$ luminosity with:

$$SFR \left[M_\odot yr^{-1} \right] = K_{H\alpha} L_{H\alpha} \left[erg \, s^{-1} \right]. \tag{4}$$

Obviously the H$_\alpha$ luminosity is deblended from the observed [NII] contribution and corrected for internal extinction as in Boselli et al. (2001). For consistency with Boselli et al. (2001) we adopt $K_{H\alpha} = 1/1.16 \times 10^{41}$ for an IMF of slope -2.5 in the mass range 0.1–80 $M_\odot$.

DM_{cont} is the dark matter contribution at the optical radius, i.e. within the 25 mag arcsec^{-2} *B* band isophote, that we assume $DM_{cont} = 0.5$, as in Kennicutt et al. (1994).

$R = 0.3$ (Kennicutt et al. 1994) is the fraction of gas that stars re-injected through stellar winds into the interstellar medium during their lifetime, that we assume $t_o \sim 12$ Gyrs.

If we assume that galaxies evolved as "closed" systems following an exponential Star Formation History (SFH), with a characteristic decay time τ since their epoch of formation (t_o), their birthrate parameter can be computed analytically (see Boselli et al. 2001) as:

$$b_{mod} = \frac{t_o \, e^{-t_o/\tau}}{\tau(1 - e^{-t_o/\tau})} \tag{5}$$

b_{mod} can be written as a function of L_H using the relation between τ and L_H found by Boselli et al. (2001):

$$\log\tau = -0.4 \, (\mathrm{Log} L_H - 12) \, [\mathrm{Gyr}] \tag{6}$$

where

$$\mathrm{Log} L_H = 11.36 - 0.4H + 2\log(\mathrm{Dist})[L_{H_\odot}]. \tag{7}$$

The dependence of b_{mod} on L_H is given as a dotted line in Figs. 8–10.

Although b and H$_\alpha$ EW have distinct dimensions, they are strongly correlated quantities. In fact they are operationally obtained in a similar way: b is computed by normalizing the H$_\alpha$ line intensity to the NIR continuum intensity, while the equivalent width is divided by the continuum intensity underlying the H$_\alpha$ line. This is shown in Fig. 3 which can be directly compared with Fig. 4 of Kennicutt et al. (1994).

4.2. The global gas deficiency parameter

For galaxies in our sample we estimate the "global gas content" $M_{gas} = M_{HI} + M_{H2} + M_{He}$.

M_{HI} is available for most (95%) targets by direct 21 cm observations (see Scodeggio & Gavazzi 1993; Hoffman et al. 1996, and references therein). The mass of molecular hydrogen can be estimated from the measurement of the CO (1–0) line emission, assuming a conversion factor (X) between this quantity and the H$_2$ surface density. X is known to vary in the range 10^{20} to 10^{21} [mol cm^{-2} (K km s^{-1})$^{-1}$] from galaxy to galaxy, according to their metallicity and UV radiation field. We adopt the empirical calibration as a function of the *H* band luminosity:

$$\log X = 24.23 - 0.38 \times \log L_H \tag{8}$$

found by Boselli et al. (2002a). The CO (1–0) line emission is unfortunately available for 52% of the considered sample
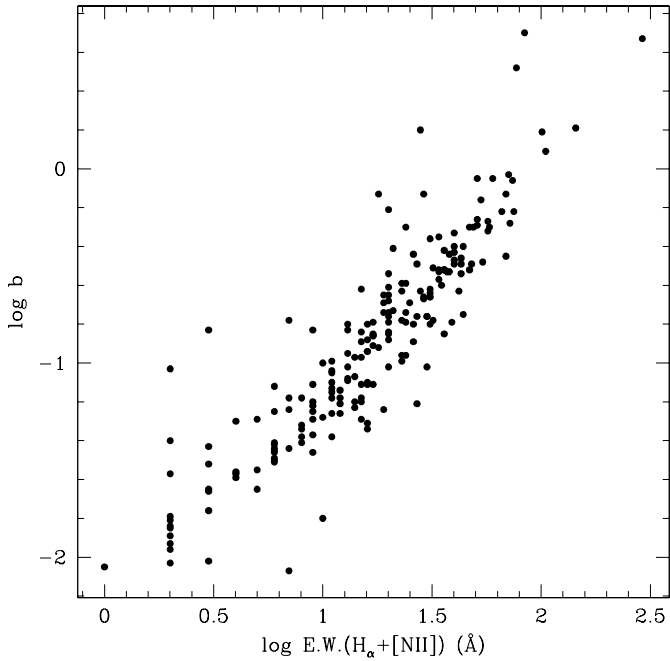
Fig. 3. The relation between the birthrate parameter and the Hα emission line equivalent width.

Fig. 4. Histograms of the Def_{gas} parameter for the isolated galaxies in the Coma supercluster (dashed line) and for Virgo galaxies (continuous line).

(see Boselli et al. 2002a and references therein), and it is assumed 15% of the HI content for the remaining objects (as concluded by Boselli et al. 2002a).

The contribution of He, not directly observable, is estimated as 30% of $M_{\mathrm{HI}} + M_{\mathrm{H2}}$ (see Boselli et al. 2002a).

We define the "gas deficiency" parameter $Def_{\mathrm{gas}} = \mathrm{Log}M_{\mathrm{gas\ ref.}} - \mathrm{Log}M_{\mathrm{gas\ obs.}}$ as the logarithmic difference between M_{gas} of a reference sample of isolated galaxies and M_{gas} actually observed in individual objects (in full analogy with the definition of HI deficiency by Giovanelli & Haynes 1985). Using a procedure similar to the one adopted by Haynes and Giovanelli (1984) we find that the gas content of 72 isolated objects in the Coma Supercluster correlates with their linear optical diameter (D): $\mathrm{Log}M_{\mathrm{gas\ ref}} = a + b\mathrm{Log}(D)$, where a and b are weak functions of the Hubble type, as listed in Table 2. Def_{gas} are listed in Col. 7 of Table 4. Histograms of the Def_{gas} parameter are given in Fig. 4 for the Coma isolated objects and for the Virgo galaxies. Isolated objects have $Def_{\mathrm{gas}} = 0 \pm 0.18$, while Virgo galaxies have significantly positive $Def_{\mathrm{gas}} = 0.53 \pm 0.35$.

5. Results

The Hα EW of galaxies is known to increase systematically along the Hubble sequence, from virtually zero for the early types (E-S0) to several hundred Å for the latest types (Kennicutt 1998). A weak trend is confirmed when data limited to the Virgo spiral galaxies included in this work are used, as shown in Fig. 5. However the scatter in each of the morphological type bins is as much as an order of magnitude, even though the scatter is somewhat reduced when gas deficient galaxies are excluded. The Hubble type alone does not account for the star formation properties of galaxies in this cluster. To shed light on other possible dependences we will analyze how the
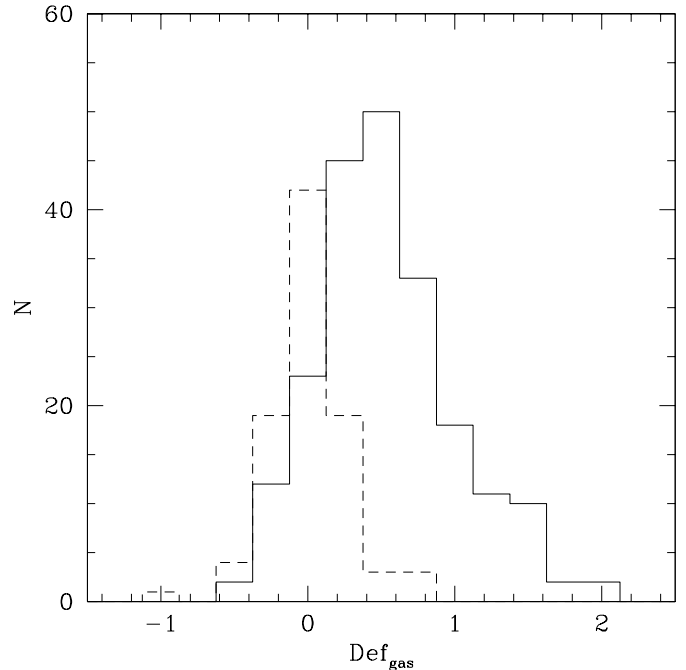
SFR varies as a function of the projected clustercentric distance (Sect. 5.1), of the luminosity (Sect. 5.2) and of the gaseous content of galaxies (Sect. 5.3).

5.1. The clustercentric dependence of the SFR

Lewis et al. (2002) analyzed the dependence of the galaxy SFR on the projected distance from clusters in the 2dF survey. Their volume limited samples comprise galaxies of all morphological types with $0.05 < z < 0.1$, brighter than $M_b < -19$. They showed with high statistical significance that the median SFR of galaxies decreases with decreasing projected distance from clusters.

It would be interesting to compare these intermediate distance clusters with the 3 local clusters analyzed in this work, however a direct comparison cannot be carried out because data of early-type galaxies are not in our possession. The dependence of the Hα EW on the clustercentric distance in units of virial radii can be analyzed only for the late-types galaxies, bearing in mind that our completeness is 60%. We compute $R_{\mathrm{virial}} = 0.002\sigma_r h^{-1}$ (Girardi et al. 1998) for the 3 clusters assuming $\sigma_r = 775, 840, 925$ km s^{-1} for Virgo, A1367 and Coma respectively.

The combined Coma and A1367 clusters (with $M_b < -19$) are shown in Fig. 6 enbedded in the Coma supercluster that we trace out to large clustercentric radial distances. We find a significant inner decrease only of the 25th percentile of the Hα EW distribution. Both the median and the 75th percentile instead increase inwards. We find it unlikely that the Hα EW distribution is biased toward high values due to incompleteness, since for the Coma+A1367 clusters our survey covers 75% of the sample. These clusters are inhabited by strong Hα emitters
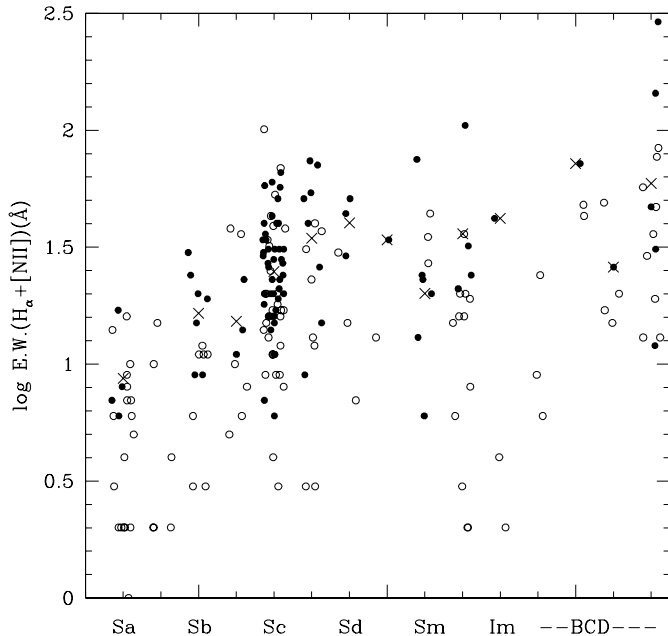
Fig. 5. The distribution of H_α EW of spiral galaxies in the Virgo cluster as a function of Hubble type. Filled dots represent galaxies with normal gas content ($Def_{gas} < 0.4$), open symbols are gas deficient objects. To avoid superposition of points, galaxies in each type bin are separated by a small random quantity. Crosses represent averages (including only the non gas-deficient galaxies) in each morphological type bin.

Fig. 6. The distribution of H_α EW as a function of (projected) cluster-centric radius from the Coma and A1367 clusters ($M_b < -19$). The top and bottom lines represent the 75th and the 25th percentile of the EW distribution, while the central line is the median of the distribution.

galaxies is occurring onto rich clusters at the present cosmological epoch.

5.2. The SFR in the Coma supercluster

Since, as concluded in the previous section, the present star formation rate of galaxies near the center of the studied clusters is a luminosity sensitive parameter, it is compelling to proceed to a systematic investigation of the luminosity dependence of the star formation properties. To this aim it is adequate to analyze the luminosity dependence of the birthrate parameter b (see Sect. 4.1). The most appropriate luminosity indicator, which we will adopt hereafter, is the NIR (H band) luminosity. This parameter traces at best the dynamical mass (within the optical disk) of spiral galaxies, as concluded by Gavazzi et al. (1996c), who found $\mathrm{Log} M_{\mathrm{dyn}} = \mathrm{Log} L_H + 0.66$.

The dependence of the b parameter on L_H, given in Fig. 8, shows that the star formation history of spiral galaxies in the Coma supercluster region is in almost inverse proportionality with the system luminosity (mass). The most massive spirals ($\mathrm{Log} L_H \sim 11.5 L_{H_\odot} \sim 12.3 \ M_\odot$) have their b parameter as much as 100 times lower than less luminous (giant) galaxies ($\mathrm{Log} L_H \sim 10 L_{H_\odot} \sim 10.8 \ M_\odot$). This confirms previous claims that the current SFR, as derived from the H_α EW, anti-correlates with the system mass (Gavazzi et al. 1998). Furthermore Fig. 8 shows that there is not a significant difference between the SFH of galaxies in the rich Coma+A1367 clusters and of relatively isolated objects in the same supercluster, in agreement with Gavazzi et al. (1998).

Both results are however biased by selection effects. The Coma supercluster galaxies were selected optically in the blue (photographic) band ($m_p \leq 15.7$). The selected targets were observed "a posteriori" in H_α and in the NIR, therefore at any given L_H only galaxies bluer than a certain threshold are sampled. In other words the B selection biases against faint-red

to which the attention has been drawn by several authors. These include the "blue galaxies in the Coma cluster" of Bothun & Dressler (1986) and the blue galaxy sample observed with ISO by Contursi et al. (2001). Many (13) galaxies with H_α EW in excess of 50 Å are found both in the inner regions ($R/R_{\mathrm{virial}} < 0.5$) and at intermediate distances ($0.5 < R/R_{\mathrm{virial}} < 1.5$) from the observed clusters. Noticeably these galaxies are near the faint limit of our survey ($-19.5 < M_b < -19$ mag).

For the Virgo cluster we separate the bright sample ($M_p < -19$), with a luminosity cutoff and H_α completeness similar to the Coma supercluster (75%), from the total sample ($M_p < -15$) and we show the two radial dependences separately in Fig. 7. The bright sample shows an inner decrease of the SFR. For the total sample this pattern no longer holds true. The Virgo cluster contains 24 galaxies with H_α EW in excess of 50 Å (11 are BCDs), the majority (14/24 objects) being fainter than -17.1 mag.

Because of their low optical luminosity the strong H_α emitters belonging to Virgo would have all escaped detection in the 2dF survey. We conclude that, beside morphology segregation, the three local clusters analyzed in this work do not show a clear radial trend of the SFR distribution. The presence of the radial trend depends purely on a luminosity cutoff, which varies cluster to cluster between -17 and -19 mag. While spiral galaxies brighter than this cutoff luminosity have lower than average SFR at the cluster centers, galaxies fainter than this limit have SFR independent from the clustercentric projected distances. This is consistent with the idea that infall of small
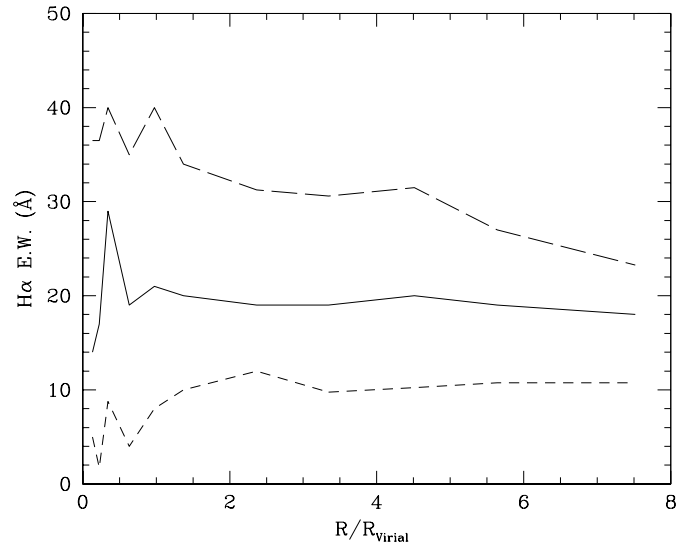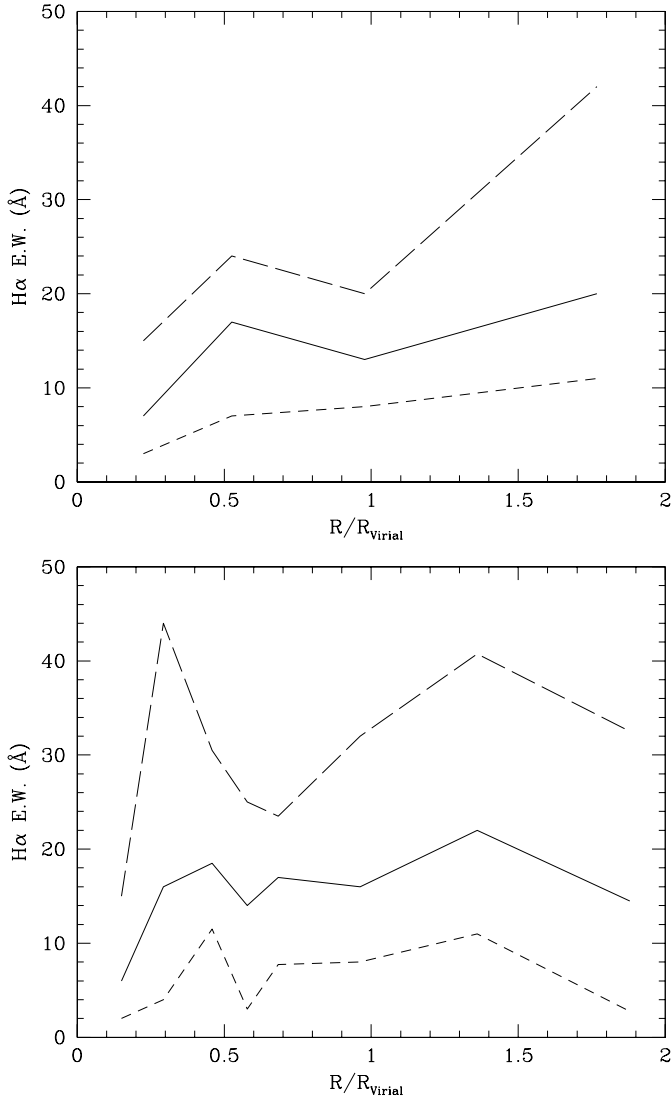
Fig. 8. The relation between the birthrate parameter and the NIR luminosity (mass) for the Coma supercluster galaxies. Galaxies in the Coma+A1367 clusters are represented with empty symbols, filled symbols are non-cluster galaxies. The dotted line represents the expected b as a function of L_H in the closed-box model of Eq. (5). The dashed line represents the observational bias affecting the Coma galaxies due to their selection in the B band.

Table 2. The M_{gas} vs. diameter relation for isolated galaxies.

Type	a	b	R^2
Sa-Sb	7.62	1.55	0.75
Sbc-Sc	7.48	1.68	0.75
Scd-Irr	7.74	1.49	0.77

Fig. 7. The distribution of H$_\alpha$ *EW* as a function of (projected) clustercentric radius from the Virgo cluster. The top and bottom lines represent the 75th and the 25th percentile of the EW distribution, while the central line is the median of the distribution. The top panel shows the Virgo galaxies brighter than $M_p = -19$, while the bottom panel includes all galaxies surveyed in H$_\alpha$ ($M_b < -15$).

galaxies, according to the relation between $B - H$ and the infrared luminosity represented by Eq. (9) (see Scodeggio et al. 2002). This, combined with the fact that b correlates with the $B - H$ color (see Eq. (10)), introduces a selection effect in the b vs. L_H plane (see Eq. (11)). These empirically determined relations are:

$$B_{\lim} - H = -12.7 - 5 \log(\text{dist}) + 2.5 \log L_H \qquad (9)$$

where $B_{\lim} = -19.2$ corresponds to the limiting magnitude ($m_p \leq 15.7$) at the Coma distance that we assume 96 Mpc.

$$\log b = 0.56 - 0.52(B - H) \qquad (10)$$

$$\log b = 7.16 + 2.6 \log(\text{dist}) - 1.3 \log L_H. \qquad (11)$$

Equation (11) is represented in Fig. 8 with a dashed line. In conclusion, faint-low star forming galaxies at the distance of
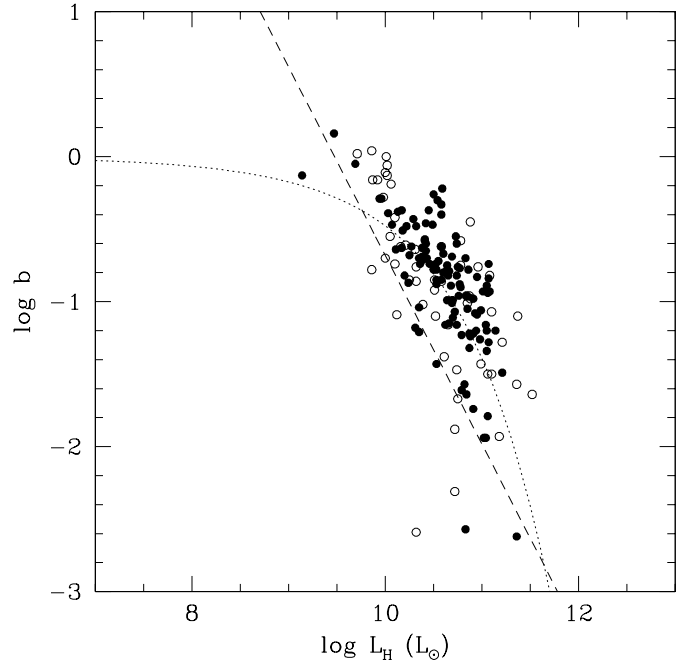
Coma below the diagonal line of Fig. 8 are severely undersampled.

5.3. The SFR in the Virgo cluster

The selection effect mentioned above affects the Virgo sample to a much lesser extent, because Virgo is 3.7 mag closer than Coma. When we consider the Virgo galaxies alone in Fig. 9 we include dwarf systems with L_H fainter by almost 2 orders of magnitudes with respect to Coma. The scatter of the b vs. L_H relation increases considerably because the large majority of faint Virgo objects have b lower than Coma. This is in agreement with Kennicutt (1983) who found evidence for significant H$_\alpha$ deficiency in 12 Virgo galaxies with respect to isolated galaxies. Galaxies with b as low as the ones in Virgo might exist in the Coma+A1367 clusters as well, but are not observed because of the previously mentioned observational bias. Thus we conclude that, at any given mass, spirals belonging to the Virgo cluster have their present star formation activity significantly lower than isolated galaxies.
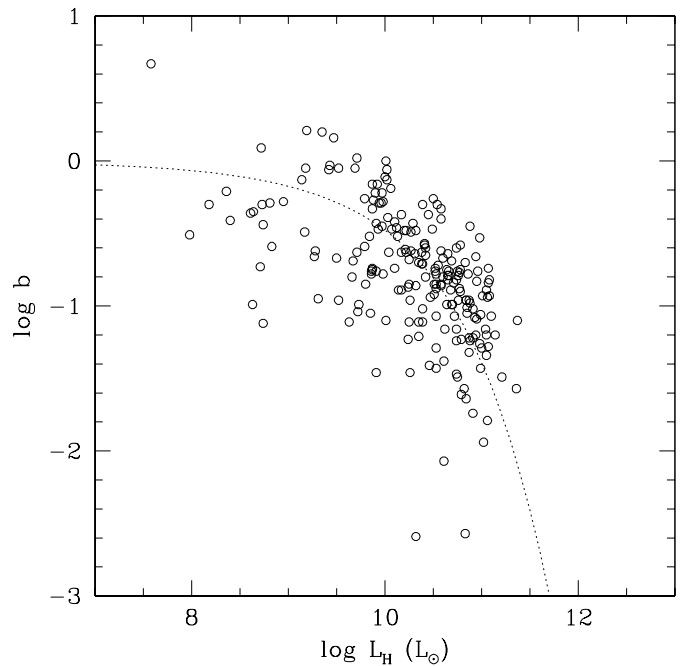
Table 3. The newly observed galaxies.

VCC/CGCG	NGC/IC	UGC	RA (*J*2000)	Dec	m_{pg}	*Vel*	T_{on}	R_{ON}
(1)	(2)	(3)	(4)	(5)	(6)	(7)	(8)	(9)
343	3148	-	121921.68	075213.8	15.1	2479	20	0.79
841	-	-	122547.40	145711.4	15.6	501	20	0.66
15031	4771	8020	125321.85	011613.5	13.3	1119	15	0.85
15049	4845	8078	125801.33	013430.3	12.9	1097	15	0.85
15055	4904	8121	130058.89	-000142.4	13.2	1174	15	0.85
41041	4116	7111	120736.33	024133.1	13.0	1309	15	0.85
43028	4688	7961	124746.67	042005.3	14.5	984	15	0.84
43034	4701	7975	124911.87	032324.5	13.1	727	15	0.79
43054	4765	8018	125314.52	042749.4	13.0	725	15	0.79
69036	4067	7048	120411.46	105114.8	13.2	2424	15	0.8
100015	4758	8014	125244.16	155050.9	14.1	1240	15	0.85
157075	-	-	115940.06	263248.7	15.7	6694	15	0.77
160121	-	8161	130329.11	263300.8	15.5	6676	20	0.77
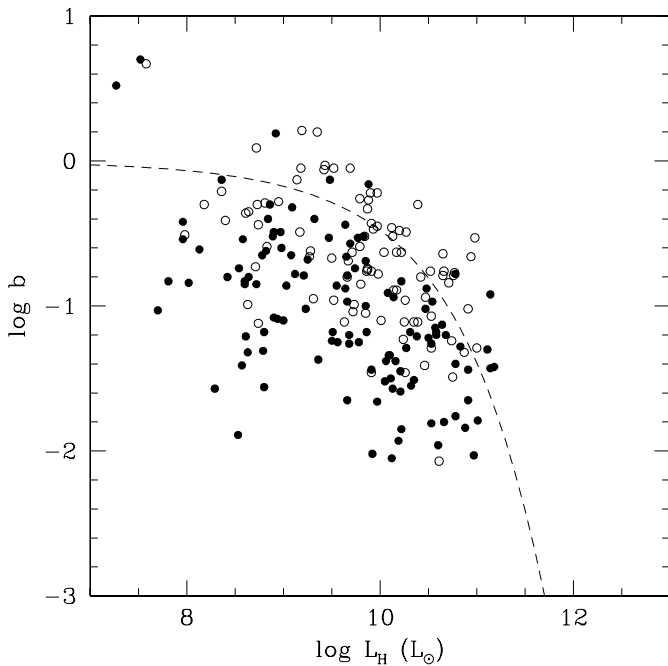
Fig. 9. The relation between the birthrate parameter and the NIR luminosity (mass) for the Virgo galaxies. Empty symbols represent galaxies with normal gas content ($Def_{gas} < 0.4$) while deficient galaxies ($Def_{gas} > 0.4$) are given with filled symbols.

Fig. 10. The relation between the birthrate parameter and the NIR luminosity (mass) for Virgo+Coma galaxies with normal gas content ($Def_{gas} < 0.4$).

It remains to be explained why. The first thing to explore is whether their gaseous content is sufficient for fueling the star formation. Cluster spirals are in fact known to suffer from HI deficiency (Giovanelli & Haynes 1985; Solanes et al. 2001), a pattern that is interpreted in the framework of the ram pressure mechanism (Gunn & Gott 1972).

When galaxies are separated according to their gas deficiency parameter (see Fig. 9), we recognize that, at any given L_H, galaxies with "normal" gas content ($Def_{gas} < 0.4$) (open symbols) have their *b* parameter significantly higher than gas "deficient" objects.

Figure 10 is restricted to the non deficient galaxies of both the Virgo and Coma regions. In this and in the previous figures the dotted curve represents b_{mod} i.e. the *b* vs. L_H relation expected from the closed-box scenario, in the assumption that τ is inversely proportional to L_H according to Eq. (6). Galaxies in Fig. 10 are found in relatively good agreement with b_{mod}, in other words their residuals $b_{obs} - b_{mod}$ are small. This is evidenced in the histograms of Fig. 11 where the distribution of
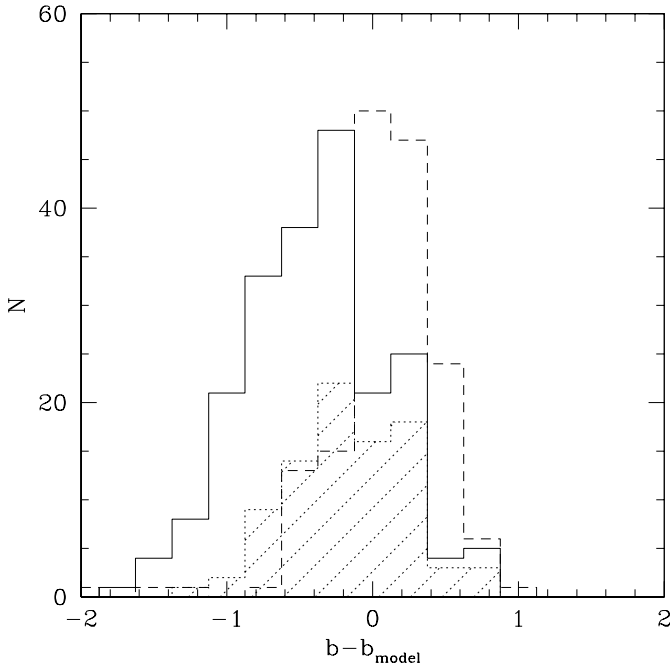
Fig. 11. Histograms of the residual $b_{obs} - b_{mod}$ for the Coma galaxies (dashed line), for Virgo (continuous line) and for the Virgo galaxies with normal HI content ($Def_{gas} < 0.4$) (dashed histogram).
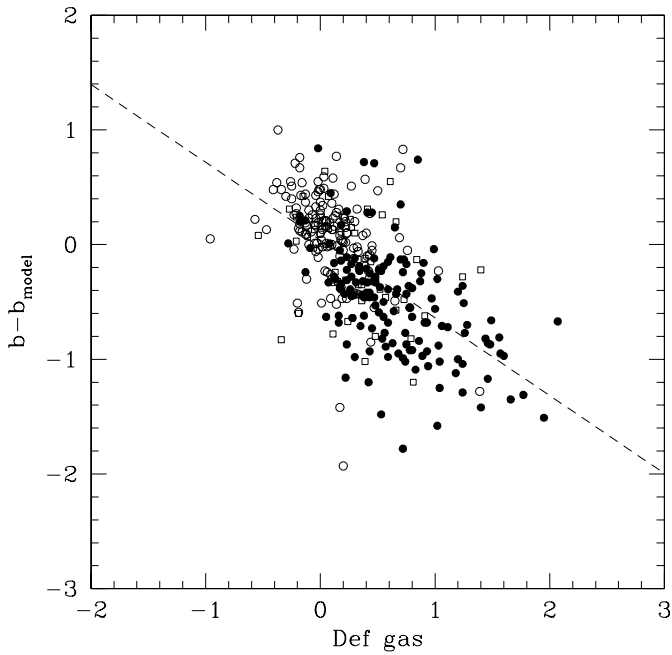

Fig. 13. The distribution of the "quenched" (empty symbols) and "healthy" (filled symbols) galaxies in the Virgo cluster. Positions of M87 and M49 are shown by crosses.

Fig. 12. The relation between $b_{obs} - b_{mod}$ and the Def_{gas} parameter. Empty circles are Coma supercluster galaxies, empty squares are "normal" Virgo clouds (N, W, S), filled circles are "deficient" Virgo clouds (A, B, E).

the residuals $b_{resid} = b_{obs} - b_{mod}$ is given separately for the Coma galaxies, for the Virgo galaxies and for the subsample of the Virgo galaxies with normal gas content ($Def_{gas} < 0.4$). Large negative residuals, implying a factor of 3 lower SFR, are associated with significantly gas deficient galaxies. It is concluded that, at any given luminosity, the principal parameter
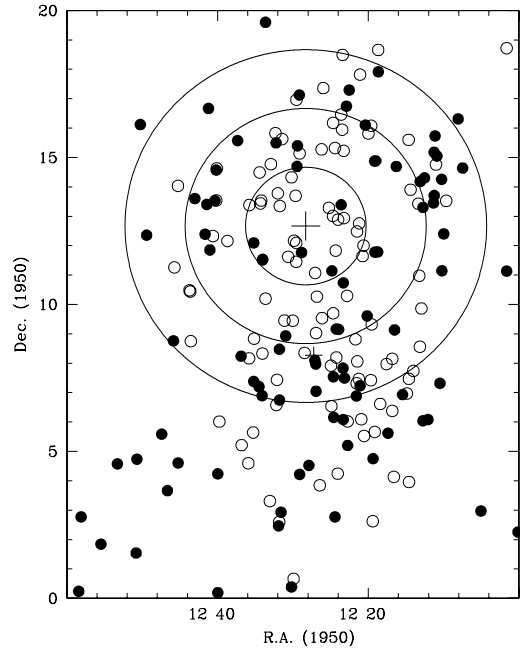
regulating the current star formation activity in cluster spirals is the availability of gas at their interior. This is further evidenced in Fig. 12, where b_{resid} is plotted against the gas deficiency parameter, showing a significant linear anti-correlation: $b_{resid} = 0.04 - 0.68 \times Def_{gas}$.

6. Discussion and conclusions

We have shown that a large fraction of late-type galaxies in the Virgo cluster have their current star formation rate significantly quenched with respect to isolated objects. These systems coincide with the Virgo gas deficient galaxies. Since the "gas" deficiency parameter is dominated by the HI phase (H_2 contributes only to 15% of the HI), it is concluded that, to the first order, the star formation properties of galaxies in the Virgo cluster are determined by the pattern of HI deficiency. As earlier recognized by Kennicutt (1998), this is a somewhat surprising result, because the typical scales of HI and of star formation are very different in disk galaxies. HI reservoirs extend some $2 \times$ the scale where the star formation takes place (Cayatte et al. 1994). We will re-examine this issue in more details in our forthcoming paper dedicated to the morphology of the star formation regions in galaxies, where a comparison between the scale-length of H_α, HI and H_2 will be carried on specifically. Limiting ourself to the global quantities, they indicate that infall of HI gas occurs in the disks on time scales similar to the star formation time. If the gas replenishment fails, because the HI reservoir is reduced by some ablation mechanism (e.g. ram pressure), the star formation adjusts itself to significantly lower rates.

Galaxies with $b_{resid} < -0.7$ and $Def_{gas} > 0.4$ ("quenched") are plotted in Fig. 13 with empty symbols, together with their "healthy" counterparts (filled symbols). Beside a marginal clustering of deficient objects around M 87 (cluster A)
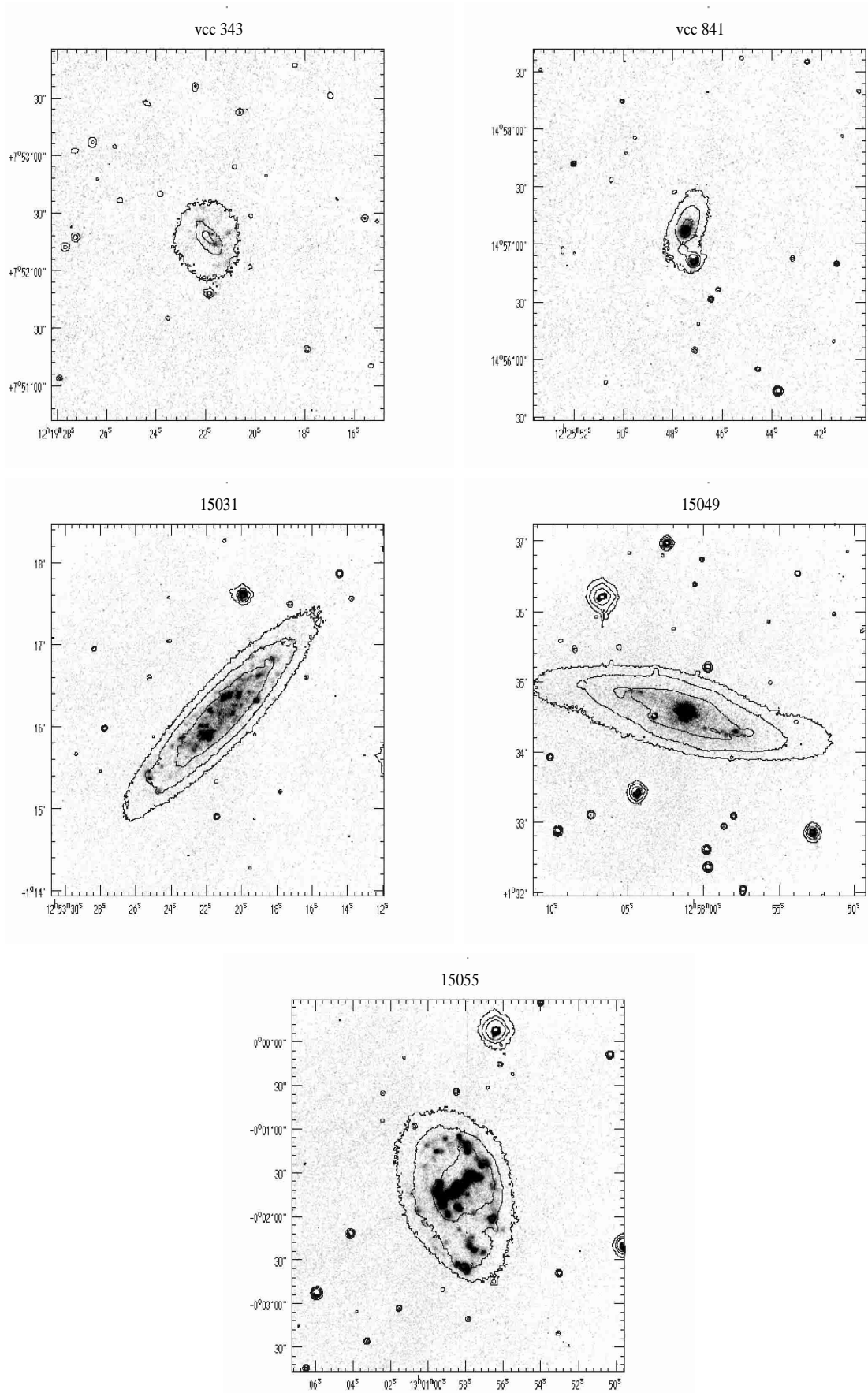
Fig. 14. Newly observed galaxies with substantial Hα + [NII] structure. The NET (ON-OFF) frames are given with grey-scale, with superposed contours of the OFF frames. J2000 celestial coordinates are given.
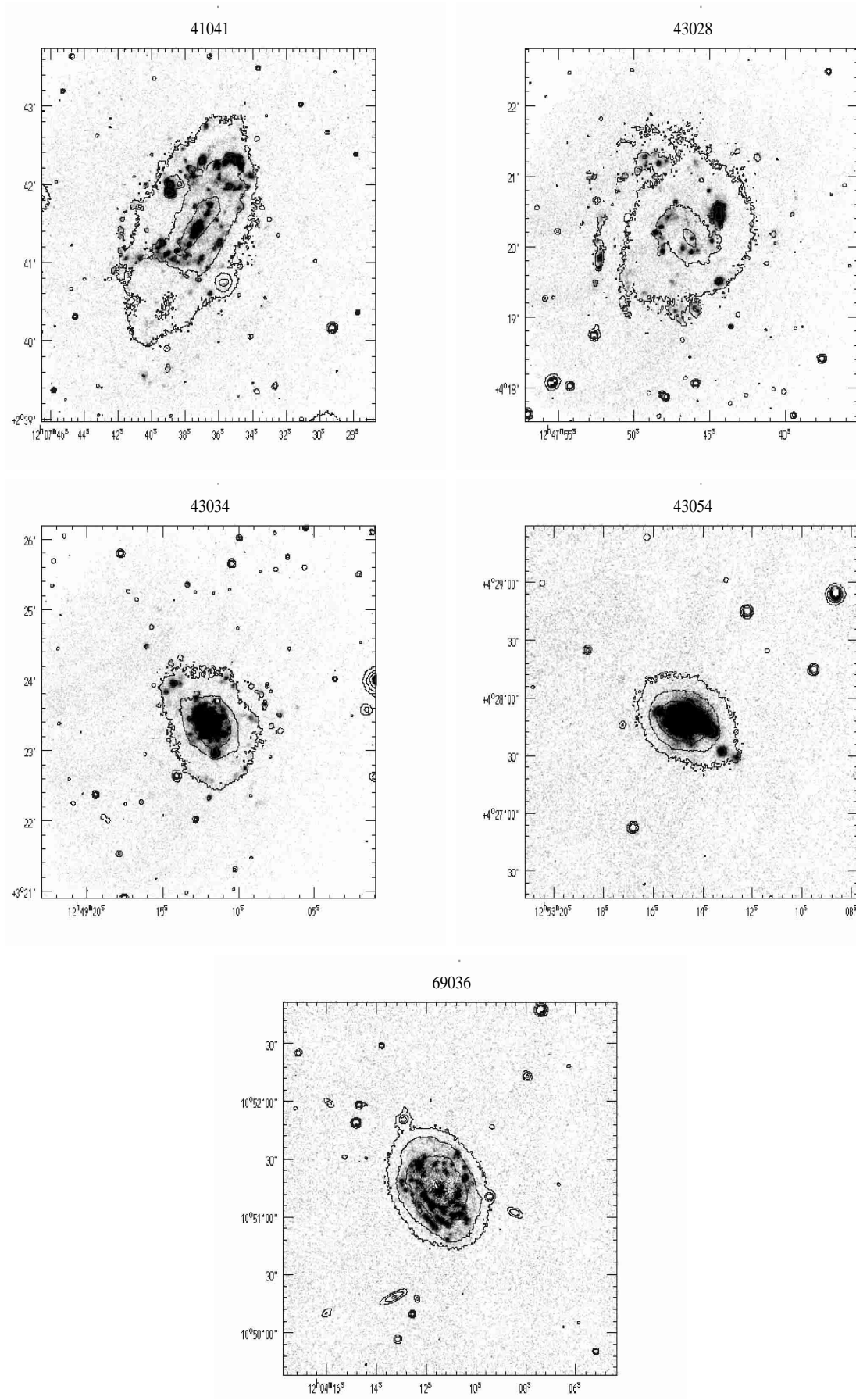
41041

43028

43034

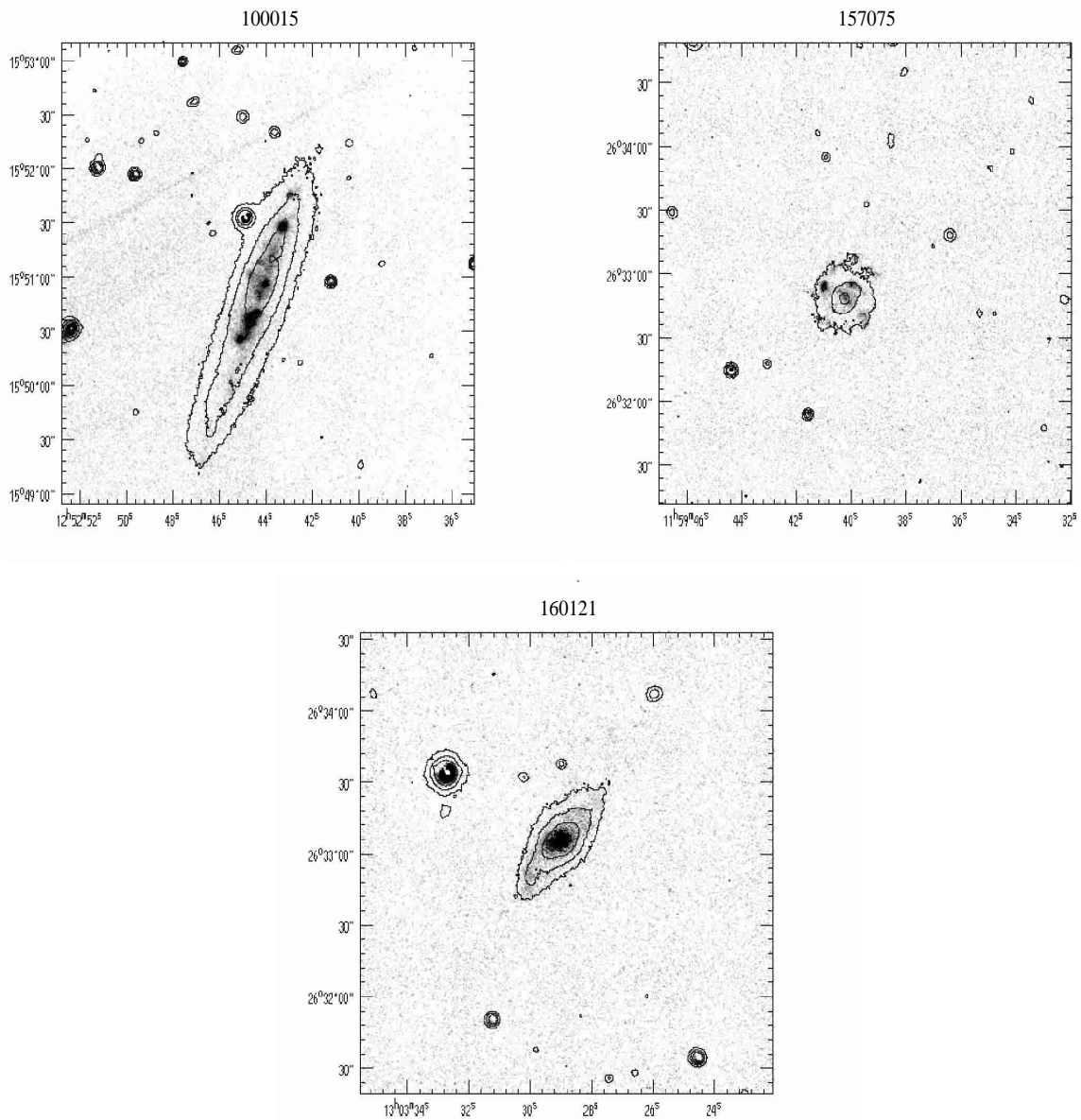43054

69036

Fig. 14. Continued.

Fig. 14. Continued.

and M 49 (cluster B) the two populations appear mixed in position. There is for example a considerable fraction of "healthy" objects projected onto the center of cluster A. However Virgo is known to be a complex dynamical entity, composed by the main cluster (A) a secondary cluster (B), several Mpc behind A, and a number of clouds at approximately the distance of A, but with significantly discrepant velocities, suggesting infall (see Gavazzi et al. 1999a).

By considering galaxies with projected angular separation <3.7 deg from M 87 we isolate 68 bona fide members of cluster A. We divide them into 48 "quenched" and 20 "healthy". For a considerable fraction (22/48 and 13/20 respectively) their distance is available from Gavazzi et al. (1999a) based on the H band Tully-Fisher relation (Tully & Fisher 1977) (distances of few galaxies whose H magnitudes were not yet available to Gavazzi et al. 1999a were recomputed by us). To our surprise we find that, while the average distance modulus of the

deficient objects (μ_o = 30.85) is in perfect agreement with the distance modulus of cluster A as a whole (μ_o = 30.82) (Gavazzi et al. 1999a), the distance modulus of the non-deficient galaxies projected onto A is μ_o = 31.77 on average, thus almost one mag more distant. It is thus concluded that "healthy" spirals projected onto the Virgo center belong in fact to a background cloud with a distance comparable with that of cluster B. This cloud has not yet entered the dense environment of cluster A.

7. Summary

– We have covered with Hα+[NII] and NIR imaging observations ~60% of the late-type (spiral) galaxies brighter than m_p = 16.0 in the Virgo cluster and in the Coma/A1367 supercluster.

– The Hα EW of spiral galaxies shows the expected decrease toward the center of the three studied clusters only when

galaxies brighter than -19.5 are considered. Weaker and dwarf systems show no or reverse trends, indicating that substantial infall of small spiral galaxies is currently taking place onto local clusters.

- From the combined Hα and NIR data we derive the birthrate, i.e. the fraction of young to old stars, providing an estimate of the star formation history for these galaxies.
- The birthrate parameter shows a weak increasing trend with increasing lateness in the Hubble classification.
- The birthrate parameter of isolated galaxies in the Great Wall is in almost inverse proportionality with the NIR luminosity, i.e. with the systemic mass. Giant spiral galaxies have a ratio of young-to-old stars 100 times lower than their dwarf counterparts.
- A large fraction of spiral galaxies in the Virgo cluster have a birthrate parameter significantly lower (a factor 3) than isolated galaxies of similar luminosity.
- Galaxies with quenched current star formation coincide with galaxies with significant gas deficiency.
- A population of currently star forming galaxies with normal gas content is found projected near the center of the Virgo cluster. Their Tully-Fisher distance is approximately 1 mag larger than the one of the deficient objects, which corresponds with the distance of the M 87 cluster. This points out the existence of a distinct cloud of galaxies falling onto the Virgo cluster.

References

Almoznino, E., & Brosch, N. 1998, MNRAS, 298, 920A
Binggeli, B., Sandage, A., & Tammann, G. 1985, AJ, 90, 1681 (VCC)
Binggeli, B., Popescu, C., & Tammann, G. 1993, A&AS, 98, 275
Boselli, A., Tuffs, R. J., Gavazzi, G., Hippelein, H., & Pierini, D. 1997, A&AS, 121, 507
Boselli, A., Gavazzi, G., Franzetti, P., Pierini, D., & Scodeggio, M. 2000, A&AS, 142, 73
Boselli, A., Gavazzi, G., Donas, J., & Scodeggio, M. 2001, AJ, 121, 753
Boselli, A., & Gavazzi, G. 2002, A&A, 386, 124 (Paper II)
Boselli, A., Lequeux, J., & Gavazzi, G. 2002a, A&A, 384, 33
Boselli, A., Iglesias, J., Vilchez, J., & Gavazzi, G. 2002b, A&A, 386, 134 (Paper III)
Bothun, G. D., & Dressler, A. 1986, ApJ, 301, 57
Cayatte, V., Kotanyi, C., Balkowski, C., & van Gorkom, J. 1994, AJ, 107, 1003
Contursi, A., Boselli, A., Gavazzi, G., et al. 2001, A&A, 365, 11
Dressler, A. 1980, ApJ, 236, 351
Gavazzi, G., Boselli, A., & Kennicutt, R. 1991, AJ, 101, 1207
Gavazzi, G., & Boselli, A. 1996, Astro. Lett. & Comm., 35, 1
Gavazzi, G., Pierini, D., Boselli, A., & Tuffs, R. 1996a, A&AS, 120, 489
Gavazzi, G., Pierini, D., Baffa, C., et al. 1996b, A&AS, 120, 521
Gavazzi, G., Pierini, D., & Boselli, A. 1996c, A&A, 312, 397
Gavazzi, G., Catinella, B., Carrasco, L., Boselli, A., & Contursi, A. 1998, AJ, 115, 1745
Gavazzi, G., Boselli, A., Scodeggio, M., Pierini, D., & Belsole, E. 1999a, MNRAS, 304, 595
Gavazzi, G., Carrasco, L., & Galli, R. 1999b, A&AS, 136, 227
Gavazzi, G., Franzetti, P., Scodeggio, M., Boselli, A., & Pierini, D. 2000b, A&A, 361, 863
Gavazzi, G., Franzetti, P., Scodeggio, M., et al. 2000a, A&A, 142, 65
Gavazzi, G., Zibetti, S., Boselli, A., et al. 2001, A&A, 372, 29
Gavazzi, G., Boselli, A., Pedotti, P., Gallazzi, A., & Carrasco, L. 2002a, A&A, 386, 114 (Paper I)
Giovanelli, R., & Haynes, M. 1985, ApJ, 292, 404
Girardi, M., Giuricin, G., Mardirossian, F., Mezzetti, M., & Boschin, W. 1998, ApJ, 505, 74
Gunn, J. E., & Gott, J. R. III 1972, ApJ, 176, 1
Haynes, M., & Giovanelli, R. 1984, AJ, 89, 758
Heller, A., Almoznino, E., & Brosch, N. 1999, MNRAS, 304, 8
Hoffman, G. L., Salpeter, E. E., Farhat, B., et al. 1996, ApJS, 105, 269
Iglesias, J., Boselli, A., Cortese, L., Vilchez, J., & Gavazzi, G. 2002, A&A, 384, 383
Kennicutt, R. 1983, AJ, 88, 483
Kennicutt, R. 1989, ApJ, 344, 685
Kennicutt, R., Tamblyn, P., & Congdon, C. 1994, ApJ, 435, 22
Kennicutt, R. 1998, ARA&A, 36, 189
Kennicutt, R., Bothun, G., & Schommer, R. 1984, AJ., 89, 1279
Kennicutt, R., & Kent, S. 1983, AJ, 88, 1094
Koopmann, R., Kenney, J., & Joung, J. 2001, ApJS, 135, 125
Lewis, I., Balogh, M., & De Propis, R. 2002, MNRAS, 334, 673
Mayer, L., Governato, F., Colpi, M., et al. 2001, ApJ, 559, 754
Moore, B., Katz, N., Lake, G., Dressler, A., & Oemler, A. 1996, Nature, 379, 613
Moore, B., Lake, G., & Katz, N. 1998, ApJ, 495, 139
Moss, C., Whittle, M., & Pesce, J. 1998, MNRAS, 300, 205
Romanishin, W. 1990, AJ, 100, 373
Scodeggio, M., & Gavazzi, G. 1993, ApJ, 409, 110
Scodeggio, M., Gavazzi, G., Franzetti, P., et al. 2002, A&A, 384, 812
Solanes, J. M., Manrique, A., Garca-Gomez, C., et al. 2001, ApJ, 548, 97
Tully, B., & Fisher, J. 1977, A&A, 54, 661
Usui, T., Saito, M., & Tomita, A. 1998, AJ, 116, 2166
Young, J., Allen, L., Kenney, J., Lesser, A., & Brooks, R. 1996, AJ, 112, 1903
Zwicky, F., Herzog, E., Karpowicz, M., Kowal, C., & Wild, P. 1961–1968, Catalogue of Galaxies and of Cluster of Galaxies (Pasadena, California Institute of Technology; CGCG)